J|A|C|S
COMMUNICATIONS

Published on Web 01/19/2007

# CVD Synthesis of Single-Walled Carbon Nanotubes from Gold Nanoparticle Catalysts

Sreekar Bhaviripudi, Ervin Mile, Stephen A. Steiner III, Aurea T. Zare, Mildred S. Dresselhaus, Angela M. Belcher, and Jing Kong*

*Department of Materials Science & Engineering, Division of Biological Engineering, Department of Physics, and Department of Electrical Engineering & Computer Science, Massachusetts Institute of Technology, Cambridge, Massachusetts 02139*

Received October 21, 2006; E-mail: jingkong@mit.edu

Single-walled carbon nanotubes (SWNTs) possess an appealing array of physical properties which give them great potential for a growing number of technological applications.[1,2] Understanding how to control the synthesis of SWNTs is vital in order to deterministically integrate such nanostructures into various technologies. To date, the most versatile techniques for synthesizing SWNTs have been those based on catalyst-assisted chemical vapor deposition (CVD). In these techniques, metal-based nanoparticles serve as catalysts in both assisting carbon feedstock cracking and facilitating the nucleation of nanotubes. In every variation of the CVD method used for synthesizing SWNTs, the composition and morphology of the catalyst nanoparticles are critical in determining the structure, length, and yield of nanotubes which will result. By far, the majority of work reporting CVD synthesis of carbon nanotubes has focused on nanoparticle catalysts based on Fe, Co, and Ni.

At the same time, there have been reports of SWNT and multiwalled nanotube growth employing catalysts based on other metals.[3−5] Exploring alternative catalysts for nanotube growth is an interesting prospect for a number of reasons. For example, NMR experiments have indicated that the ratio of metallic to semiconducting SWNTs grown with Co/Ni-based catalysts is different than when Rh/Pd catalysts are used.[6] This suggests that it may be possible to change the ratio of metallic to semiconducting nanotubes by varying the catalyst composition. In addition, at present in the field of nanotube research, there is no clear understanding regarding the important factors for catalyzing nanotube growth. Based on the evaluation of carbon solubility and carbide stability from the carbon−metal binary phase diagrams, it has been suggested that Fe, Co, and Ni are the only elements capable of catalyzing SWNT growth among 70 elements that include all of the transition metals.[7] However, this is contradicted by experimental results. Therefore, a detailed comparison between the similarities and differences of various metal catalysts will help to elucidate the growth mechanism in greater depth.

Gold is one potentially interesting alternative to Fe, Co, and Ni. Bulk gold has historically been regarded as relatively inactive toward catalyzing chemical reactions due to its completely filled 5d shell and relative high first ionization energy.[8] Over the past decade, however, it has been shown that nanoscale gold particles possess enhanced catalytic activity over their bulk counterpart due to size effects.[4,9] Additionally, bulk Au has a melting point of 1064 °C, and so, due to size effects, Au nanoparticles of diameters suitable for SWNT growth are expected to have melting points as low as 300 °C.[10] This low melting point may enable lower CVD growth temperatures than is possible with Fe, Co, and Ni under otherwise identical conditions, advantageous for the direct integration of nanotubes into different technologies with temperature-limiting materials.

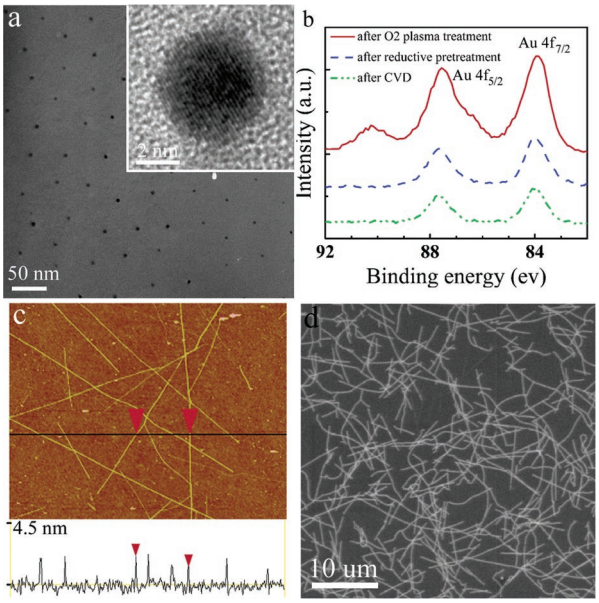


***Figure 1.*** (a) TEM image showing monodisperse Au nanoparticles. (b) High-energy resolution XPS spectra of Au nanoparticles at different stages of treatment. (c) A typical AFM height image (5.0 × 3.9 $\mu m^2$) and the corresponding cross-sectional image. (d) SEM image of nanotubes grown from Au catalysts.

In this paper, we present the first demonstration of SWNT growth by thermal CVD employing gold nanoparticles. Growth was carried out using highly monodisperse Au nanoparticle catalysts prepared by block copolymer templating technique.[11] Synthesis of SWNTs and MWNTs from catalysts prepared using block copolymer templates have been recently reported.[12−14] In a typical experiment, 0.2 g of polystyrene−poly(4-vinylpyridine) (PS−P4VP) diblock copolymer is dissolved in 50 mL of toluene to form reverse micelles in toluene consisting of polar P4VP cores in nonpolar PS domains.[11] Two milligrams of tetrachloroauric acid ($HAuCl_4 \cdot 3H_2O$) is added to the solution. Interactions between the Au salt and pyridine unit of the PS−P4VP sequester Au ions within the spherical micellar domains. The Au-loaded polymer micellar solution is then spin-coated onto $Si/SiO_2$ substrates to form a monolayer of micelles. Subsequently, $O_2$ plasma treatment is carried out to remove the polymeric shell. Figure 1a is a transmission electron microscopy (TEM) image of the Au nanoparticles. The lattice fringes from a gold nanocrystal are seen in the inset.

The syntheses of SWNTs were carried out in a 2.5 cm diameter quartz tube furnace. Typically, substrates with Au nanoparticles (after $O_2$ plasma treatment) were loaded into the quartz tube and heated to growth temperature (800 or 900 °C) under Ar flow. At


10.1021/ja0673332 CCC: $37.00 

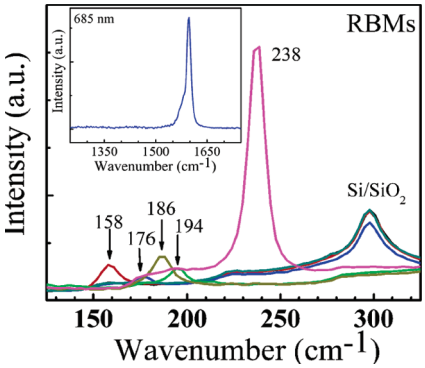


***Figure 2.*** Raman spectra of the nanotube sample grown with the Au catalyst. The inset shows the G-band and the absence of D-band.

the growth temperature, the flow of Ar was replaced by a flow of 440 sccm $H_2$ and maintained for 15 min to reduce the nanoparticles. Subsequently, the synthesis was initiated by introducing a flow of 20 sccm $C_2H_4$, 30 sccm $CH_4$, and 440 sccm $H_2$ for 10 min. After growth, the hydrocarbon gases were turned off, the tube was removed from the furnace, and a flow of 600 sccm Ar was activated as the tube cooled to room temperature.

Numerous trials were performed to evaluate the influence of various process parameters on nanotube yield. It was found that no growth would occur without a reductive pretreatment, and that a process temperature of 800 °C resulted in a higher yield than 900 °C. Figure 1b shows the high-resolution X-ray photoelectron (XPS) spectra of Au nanoparticles after $O_2$ plasma, after reductive pretreatment, and finally after CVD. Two chemistries of gold are observed prior to the reductive pretreatment, with the higher binding energy possibly attributable to either a residual shell of gold chloride or gold oxide (as a result of plasma treatment) on the nanoparticles. These higher binding energy chemistries disappear after the reductive pretreatment, suggesting that the $H_2$ treatment successfully removes this residual material. Given the inability of unreduced particles to successfully catalyze nanotube growth, it can be concluded that the presence of these higher binding energy chemistries of gold somehow inhibits nanotube growth.

The presence of densely populated nanotubes on the surface of the substrate after CVD at 800 °C as shown in a representative scanning electron microscopy (SEM) image (Figure 1d) indicates that Au serves as an efficient catalyst. Atomic force microscopy (AFM) height images of nanotubes reveal that the growth of nanotubes occurs from individual catalyst nanoparticles with diameters ranging from 1 to 2 nm (Figure 1c). Resonant Raman spectra of nanotubes were collected using a laser excitation wavelength of 685 nm. The presence of radial breathing modes (RBM) in the spectra at various spots on the surface verifies that these structures are SWNTs (Figure 2). Using the relationship for nanotube diameter $d_t$ (nm) = 233 $cm^{-1}/\omega_{RBM}$,[15] the diameters of the SWNTs are found to be between 1.2 and 1.8 nm, consistent with the AFM height measurements. In addition, the absence of disorder-induced Raman mode (D-band) at around 1300 $cm^{-1}$ indicates the high quality of as-grown SWNTs (inset of Figure 2).

Interestingly, a decrease in the density of the gold nanoparticles on the substrate is observed after CVD. This could be due to either evaporation of gold from the substrate (as a result of the low melting point of the Au nanoparticles) or possibly the diffusion of gold into the substrate. Further investigation will be carried out to understand this phenomenon. In addition, the average diameter of the nanoparticles (as measured by AFM) appears to decrease from $3.1 \pm 0.4$ nm to ~2.0 nm (see Supporting Information). This could again be due to the evaporation of gold from the substrate or reduction of the oxide shell. At present, our attempts to grow SWNTs at temperatures lower than 800 °C using thermal CVD have not been successful. We believe this is mainly due to the thermal energy required for cracking the carbon feedstock. A two-stage furnace or other means to decompose the hydrocarbon gases, such as hot-filament CVD or plasma-enhanced CVD,[16] may eventually lead to a lower growth temperature with Au nanoparticle catalysts.

In summary, the growth of SWNTs using gold nanoparticle catalysts was successfully demonstrated. Investigations are currently underway to achieve low-temperature SWNT growth. Furthermore, a detailed analysis with resonant Raman spectroscopy[17] will be carried out to elucidate the metallic to semiconducting ratio of the SWNTs. Given the increased interatomic distance of Au over Fe, Co, or Ni, it is possible that the chirality distribution of SWNTs grown from the Au nanoparticles could be different from those of conventional catalysts. Our successful synthesis opens up the route for the investigation of chirality modification through parameter control during the CVD.

**Acknowledgment.** We thank Hyungbin Son, Hootan Farhat, and Jifa Qi for helpful discussions. This work was supported by grants from MARCO-FENA and MARCO-IFC. Raman measurements were carried out in Spectroscopy Laboratory supported by NSF-CHE 0111370 and NIH-RR02594 grants.

**Supporting Information Available:** Experimental details for nanoparticle synthesis, size distribution, and XRD data. This material is available free of charge via the Internet at http://pubs.acs.org.

## References

(1) Tans, S. J.; Verschueren, A. R. M.; Dekker, C. *Nature* **1998**, *393*, 49−52.
(2) Fuhrer, M.; Park, H.; McEuen, P. L. *IEEE Trans. Nanotechnol.* **2002**, *1*, 78−88.
(3) Lee, C. J.; Lyu, S. C.; Kim, H.-W.; Park, J. W.; Jung, H. M.; Park, J. *Chem. Phys. Lett.* **2002**, *361*, 469−472.
(4) Lee, S. Y.; Yamada, M.; Miyake, M. *Carbon* **2005**, *43*, 2654−2663.
(5) Wal, R. L.V.; Ticich, T. M.; Curtis, V. E. *Carbon* **2001**, *39*, 2277−2289.
(6) Tang, X.-P.; Kleinhammes, A.; Shimoda, H.; Fleming, L.; Bennoune, K. Y.; Sinha, S.; Bower, C.; Zhou, O.; Wu, Y. *Science* **2000**, *288*, 492−494.
(7) Deck, C. P.; Vecchio, K. *Carbon* **2006**, *44*, 267−275.
(8) Bailar, J. C. *Comprehensive Inorganic Chemistry*; Pergamon: New York, 1973; Vol. 1, p 129.
(9) Schmid, G. *Chem. Rev.* **1992**, *92*, 1709−1727.
(10) Buffat, P.; Borel, J.-P. *Phys. Rev. A* **1976**, *13*, 2287−2296.
(11) (a) Spatz, J. P.; Mossmer, S.; Hartmann, C.; Moller, M. *Langmuir* **2000**, *16*, 407−415. (b) Glass, R.; Moller, M. Spatz, J. P. *Nanotechnology* **2003**, *14*, 1153−1160.
(12) Lu, J.; Yi, S. S.; Kopley, T.; Qian, C.; Liu, J.; Gulari, E. *J. Phys. Chem. B* **2006**, *110*, 6655−6660.
(13) Bhaviripudi, S.; Reina, A.; Qi, J.; Kong, J.; Belcher, A. M. *Nanotechnology* **2006**, *17*, 5080−5086.
(14) Bennett, R. D.; Hart, A. J.; Cohen, R. J. *Adv. Mater.* **2006**, *18*, 2274−2279.
(15) Kurti, J.; Zolyomi, V.; Kertesz, M.; Sun, G. *New J. Phys.* **2003**, 5, 125.1−125.21
(16) Li, Y.; Mann, D.; Rolandi, M.; Kim, W.; Ural, A.; Hung, S.; Javey, A.; Cao, J.; Wang, D.; Yenilmez, E.; Wang, Q.; Gibbons, J. F.; Nishi, Y.; Dai, H. *Nano Lett.* **2004**, *4*, 317−321.
(17) Son, H. B.; Reina, A.; Dresselhaus, M. S.; Kong, J. *Phys. Status Solidi B* **2006**, *243*, 3161−3165.

JA0673332